IN-02
48310
P 9

NASA Technical Memorandum 106919

# A Combined Geometric Approach for Solving the Navier-Stokes Equations on Dynamic Grids



John W. Slater
*Lewis Research Center*
*Cleveland, Ohio*

Prepared for the
Conference on Numerical Methods for Fluid Dynamics
sponsored by the University of Oxford and Reading
Oxford, England, United Kingdom, April 3–6, 1995

National Aeronautics and
Space Administration

# A Combined Geometric Approach for Solving the Navier-Stokes Equations on Dynamic Grids

John W. Slater [1]
NASA Lewis Research Center, Cleveland, Ohio, USA

**Abstract**

**A combined geometric approach for solving the Navier-Stokes equations is presented for the analysis of planar, unsteady flow about mechanisms with components in moderate relative motion. The approach emphasizes the relationships between the geometry model, grid, and flow model for the benefit of the total dynamics problem. One application is the analysis of the restart operation of a variable-geometry, high-speed inlet.**

## 1 Introduction

The computation of the unsteady flow about mechanisms with components in relative motion has become an important topic in computational fluid dynamics (CFD) (Mani and Haney 1994, Atwood 1994, Wang and Yang 1994, Trépanier *et al.* 1993). One such mechanism is the NASA Variable Diameter Centerbody (VDC) inlet in which the axisymmetric centerbody can translate and change diameter to adjust the mass flow rate and stabilize the flow.

When the components of the mechanisms are in relative motion, the geometry modeling, grid generation, and flow modeling aspects of the CFD analysis process all become functions of time. The combined geometric approach emphasizes the geometry model and its relationship with the grid and flow model for the benefit of the total dynamics problem. The following sections discuss the approach and present some applications to demonstrate the concepts and performance.

## 2 Geometry Modeling

The geometry model is constructed of geometric entities representing each component of the mechanism. This allows for accurate modeling of the mechanism and specification of the component kinematics. The work presented here considers a planar geometry model as would be needed for a two-dimensional or axisymmetric CFD analysis. Each geometric entity is represented mathematically as either a linear or cubic spline curve using a parametric coordinate corresponding to the arclength along the entity. Each component is assumed to move only as a rigid body. Thus, the geometric entities only require modeling at the start of the computation. During the computation, geometric information is obtained from the geometry model as a function of the geometric entity, parametric coordinate, and time. The information includes: the position, velocity, tangent, normal, acceleration, second-derivative, and curvature.

A mechanism used to illustrate the concepts is the NASA Variable Diameter Centerbody (VDC) inlet (Saunders and Linne 1992). The VDC inlet is a mixed-compression, high-speed inlet designed to operate at a Mach number of 2.5 with a 45% internal compression using a biconic centerbody. The second and aft

[1] National Research Council Associate, CFD Branch, Internal Fluid Mechanics Division

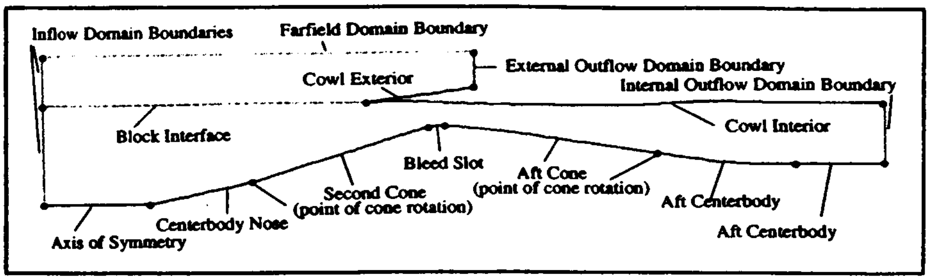


FIG. 1. The planar geometry model of the NASA VDC inlet.

cones of the centerbody consist of overlapping leaves which form an umbrella mechanism which allows the diameter of the centerbody to change to vary the mass flow of air entering the inlet. The centerbody may also translate. Figure 1 shows the planar geometry model with the individual entities identified.

The change in diameter of the centerbody is modeled by specifying the rotation of the geometric entities defining the second and aft cones about their respective points of rotation. The translation of the centerbody is modeled by specifying the translation of the geometric entities defining the centerbody.

Included in the geometry modeling is the domain modeling in which a boundary is created to define the enclosed space which becomes the flow domain. The boundary will consist of the geometric entities and domain boundary entities. The domain boundary entities are mathematically defined in the same manner as the geometric entities. In Fig. 1, the domain boundary entities include the inflow, farfield, and outflow entities. The relative motion of some of the geometric entities requires that some domain boundary entities be of variable geometric representation. In Fig. 1, the bleed slot entity will be of variable representation as the second and aft cones rotate.

## 3 Grid Generation

The motion of the geometric entities means that the grid may require some regeneration each time step. This requires an efficient grid generation approach. A multi-block, structured grid topology is used with grid lines matching contiguously across blocks. This topology provides for accurate and efficient computation of turbulent, viscous flows. Further, the moderate levels of component motion did not warrant a more complex topology.

The topology of a block is defined by specifying the entities of the geometry model which comprise the faces of the blocks. The boundary between blocks is defined by a block interface, which is represented in the same mathematical form as the geometric and domain boundary entities and is considered part of the geometry model. The topology of the block is assumed to remain fixed throughout the computation. This imposes a limitation on the extent of the motion of the entities, but it allows for efficient grid generation.

Quality dynamic grids are efficiently obtained by dividing a block into smaller

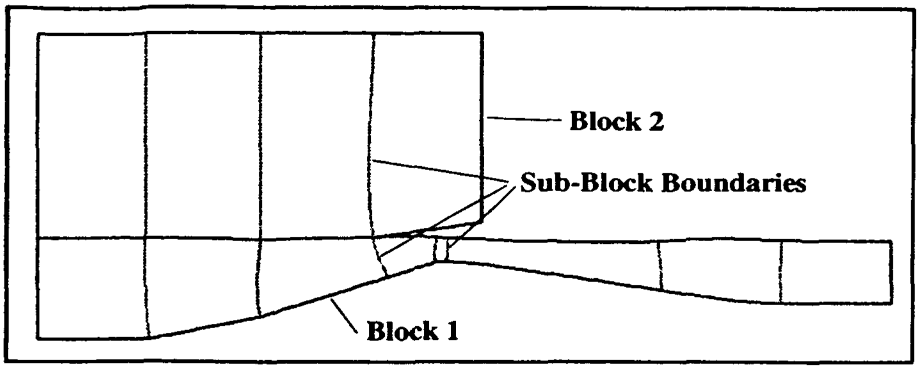


FIG. 2. The block and sub-block boundaries for the grid for the VDC inlet.

sub-blocks according to the geometric features of the entities. Also, the amount of regeneration of the grid can be minimized to include only those sub-blocks having dynamic boundaries. The shape of a sub-block boundary is defined using a two-point cubic spline with the endpoint tangents specified by the normal vectors of the entities at the endpoints. Figure 2 shows how the flow domain for the VDC inlet is divided into two blocks with sub-blocks. The orthogonality of the sub-block boundary curves at the entities can be seen. This results in an interior grid which also has orthogonality.

An automated procedure determines the grid density and spacing along the boundary of the sub-block based on global grid quality parameters such as minimum and maximum grid spacing and maximum grid spacing ratio, the geometry model, and the flow boundary conditions. Local grid quality parameters associated with entities can also be specified. A hyperbolic tangent method is then used to distribute the grid points along the boundaries. Using the geometry model assures that the boundary grid points are placed on the entities and the dynamics of the boundary grid points are precisely defined.

The generation of the volume grid and grid dynamics is performed efficiently through the use of an algebraic, transfinite interpolation method applied for each sub-block. Only those sub-blocks with motion over a time step require regeneration. Several strategies exist for generating the dynamic grid. First, the grid coordinates can be regenerated with grid speeds computed through a backwards time difference. One problem is how to compute grid speeds at the starting time of the computation when no previous grids exist. Also, the grid dynamics may lag the geometry dynamics. A second strategy involves using grid deformations on the boundary to compute interior deformations using a transfinite interpolation. This is essentially the same as the first strategy, but may be a better numeric formulation depending on the finite-volume approximation. The third strategy involves using the boundary grid speeds to compute the interior grid speeds through a transfinite interpolation. The grid is then obtained through a time integration. This has the advantage that grid speeds can be computed at the starting time and represent the current motion of the geometry. An example

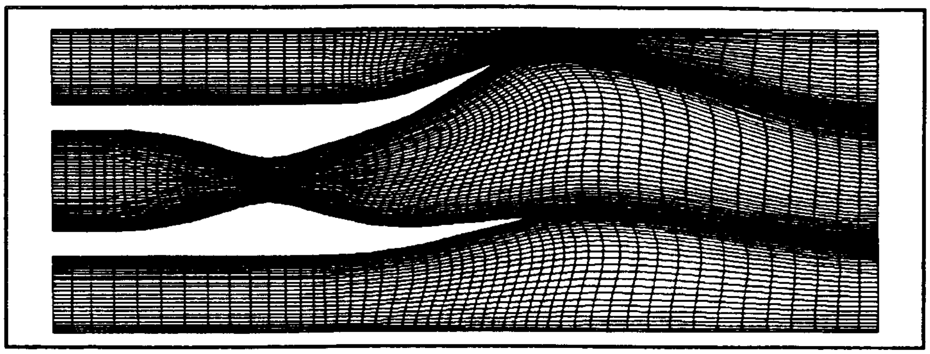

FIG. 3. A grid for a thrust-vectored nozzle.

of the application of the grid generation approach is shown in Fig. 3.

## 4 Flow Modeling

The Navier-Stokes equations for a time-varying control volume are

$$\hat{U}_t + \hat{R} = 0 \tag{4.1}$$

where

$$\hat{U} = \int_{V(t)} U \, dV \quad \text{and} \quad \hat{R} = \oint_{S(t)} \mathbf{H} \cdot \hat{n} \, dS.$$

The $U$ is the algebraic vector of conservative variables $U^T = ( \rho, \rho u, \rho v, E_t )$ where $\rho$ is the density and $u$ and $v$ are the flow velocity Cartesian components. The $E_t$ is the total energy per unit volume. The $V$ is the volume and $S$ is the surface area. The $\hat{n}$ is the surface normal vector. The $\mathbf{H}$ is the flux dyadic, which for a mixed Eulerian-Lagrangian description (Vinokur 1989) is,

$$\mathbf{H} = \mathbf{F} - \vec{g}\, U. \tag{4.2}$$

The $\vec{g}$ is the velocity vector of the control surface, $\vec{g} = x_\tau \hat{\imath} + y_\tau \hat{\jmath}$. An Eulerian description is obtained for $\vec{g} = 0$ while a Langrangian description is obtained for $\vec{g} = \vec{V}$. The $\mathbf{F}$ is the Cartesian flux dyadic. The flow model is complete with Sutherland's formula, the definition of the Prandtl number, a perfect gas assumption, Reynolds averaging, and the Baldwin-Lomax turbulence model.

The approach associates the flow boundary conditions with the geometry model entities. For example, the entities representing the centerbody are specified as solid wall boundary conditions. The flow boundary condition modeling makes use of the geometry model. Consider the physical condition for a slip wall,

$$\rho \left( \vec{V} - \vec{g} \right) \cdot \hat{n} = \dot{m}, \tag{4.3}$$

where $\dot{m}$ is the mass flux. The surface normal vector $\hat{n}$ is computed from the geometry model rather than the local grid. Other flow boundary condition models use the wall tangent vector and curvature computed from the geometry model.

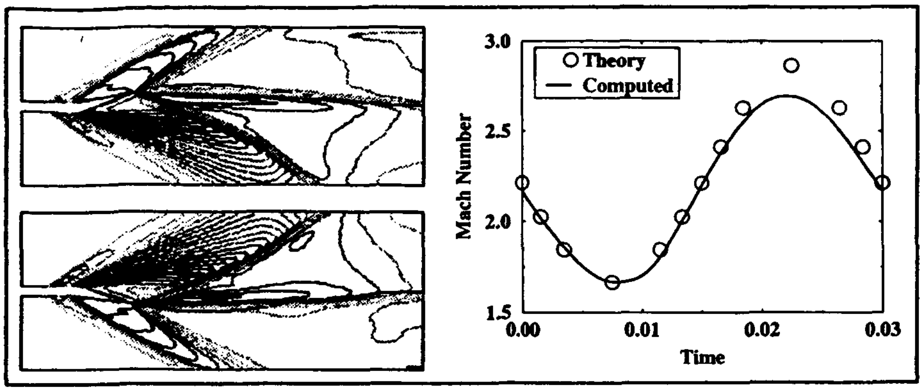


FIG. 4. A simple hinged flap.

## 5 Time-Dependent Computation of the Dynamics

A cell-vertex, finite-volume approximation is used for the spatial discretization of eqn 4.1. The temporal discretization uses an explicit, two-stage Lax-Wendroff method (Liou and Hsu 1989) of the form

$$\hat{U}^{*} = \hat{U}^{n} + \Delta\tau\, \hat{R}^{n}, \tag{5.1}$$

$$\hat{U}^{**} = \hat{U}^{*} + \Delta\tau\, \hat{R}^{*}, \tag{5.2}$$

and

$$\hat{U}^{n+1} = (\hat{U}^{n} + \hat{U}^{**})\,/\,2. \tag{5.3}$$

The inviscid fluxes are computed using the Roe flux-difference splitting with a TVD limiter. The viscous fluxes are computed using differences and averages computed at the cell faces. The $V$ needed to decode $\hat{U}$ is computed from the geometric conservation law (Thomas and Lombard 1979) which relates the change in volume of the cell to the motion of the cell faces. The geometric conservation law for the explicit method follows the form of eqns 5.1 to 5.3 with $\hat{U} = V$ and $\hat{R} = \hat{Z}$ where $\hat{Z}$ is the vector sum of the speeds of the cell faces.

## 6 Application: Simple Hinged Flap

A simple mechanism is a flat plate with a flap which rotates about its hinge in a sinusoidal manner with an amplitude of 15 degrees and a period of 0.03 seconds. An inviscid flow analysis with a freestream Mach number of 2.0 was performed. As the flap rotates, oblique shock waves and corner expansion fans develop and dissipate. The computed Mach numbers on the flap surface can be compared to those from steady-state, inviscid theory to obtain some evaluation of accuracy. As can be seen in figure 4, the compressions compared well, but during the expansions, the Mach number was slightly less than theory. The fluid and flap motion time scales were of the same order of magnitude and dynamic effects may have been more significant in the expansion process.

The performance of dynamic grids for the computation of turbulent, viscous flow was examined for a hinged-flap for a Reynold's number of $1.0 \times 10^6$. The flap was set to rotate sinusoidally for an amplitude of 20 degrees with a time period of 0.01 seconds for three time periods. The amount of CPU usage required for the computation depends on the level of grid dynamics, which can be computed as the time average of the percentage of grid points that are regenerated for the time interval of the computation. For the flap analysis, the grid dynamics level was 71%. At this grid dynamics level, the increase in the CPU usage was about 31% over the CPU usage required for a computation on a static grid.

## 7 Application: Restart of the NASA VDC Inlet

In normal cruise operations of the VDC inlet, a normal shock is positioned just aft of the throat. Flow disturbances can cause the shock to move forward of the throat and unstart the inlet. The restart of the inlet involves a forward translation and reduction of the diameter of the centerbody and an opening of the bypass doors to reduce the back pressure at the compressor face.

An inviscid, axisymmetric flow analysis demonstrates the importance of the variable geometry in the analysis of the restart process. The freestream Mach number was 2.5 with a compressor face Mach number of 0.31. An impulse in the Mach number of a magnitude of - 0.12 was applied at the compressor face over a time interval of 0.01 seconds. The shock moved forward of the throat and the inlet was unstarted. At $t = 0.04$ seconds the restart was initiated. The centerbody translated a distance of 0.2 units forward and the second cone rotated from an angle of 18.5 degrees to an angle of 12.5 degrees, which is equal to the angle of the nose cone. The time interval of the centerbody motion was 0.04 seconds. The compressor face Mach number was increased from a value of Mach 0.31 to 0.50 over a time interval of 0.01 seconds to simulate the reduction of the back pressure. At $t = 0.15$ seconds, the normal shock returned to the diffuser and the inlet was returned to normal operating conditions. Figure 5 shows the sequence of Mach number contours for the unstart / restart process.

The amount of diameter change required to restart the inlet was greater than that reported in the wind tunnel tests. This may be due to the limitations of the inviscid analysis. It was determined that the dynamic grid generation increased the amount of CPU usage by about 21% for a dynamic grid level of 24% for the time interval starting from the initiation of the restart process. Other analyses were performed and it was determined that the inlet could not restart without moving the centerbody, regardless of the level of reduction of the back pressure.

## 8 Conclusions

The combined geometric approach provides a natural formulation of the total dynamics problem for dynamic grid CFD analysis methods. The geometry modeling and grid generation become more important for dynamic geometries and their relationship with the flow modeling can be used effectively for the benefit of the total dynamics problem.

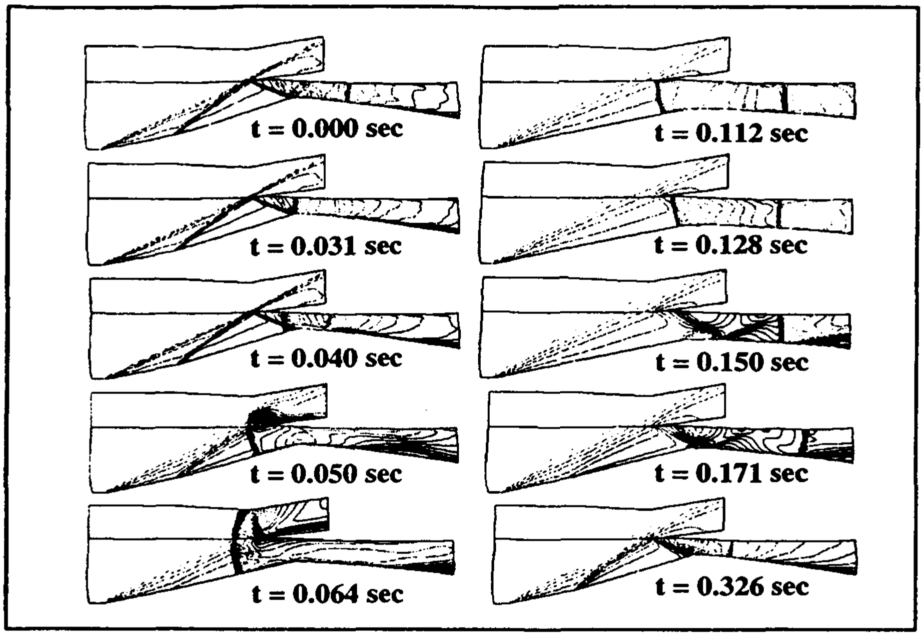


FIG. 5. Sequence of Mach number contours for the inviscid flow during the unstart / restart process of the VDC inlet with centerbody motion.

## Bibliography


1. Atwood, C.A. (1994). "Computation of a Controlled Store Separation from a Cavity." AIAA-94-0031.
2. Liou, M.-S. and Hsu, A.T. (1989). "A Time-Accurate Finite Volume High Resolution Scheme for Three Dimensional Navier-Stokes Equations." AIAA-89-1994.
3. Mani, K.K. and Haney, J.W. (1994). "3D CFD Analysis of a SR71-Waverider Launch Configuration." AIAA-94-0156.
4. Saunders, J.D. and Linne, A.A. (1992). "Status of the Variable Diameter Centerbody Inlet Program." NASA CP-10087, 1481-1504.
5. Thomas, P.D. and Lombard, C.K. (1979). "Geometric Conservation Law and its Application to Flow Computations on Moving Grids." *AIAA Journal*, **17**, 1030-37.
6. Trépanier, J.Y., M. Reggio, M. Paraschivoiu, and R. Camarero (1993). "Unsteady Euler Solutions for Arbitrarily Moving Bodies and Boundaries." *AIAA Journal*, **31**, 1869-76.
7. Vinokur, M. (1989). "An Analysis of Finite-Difference and Finite-Volume Formulations of Conservation Laws." *Journal of Computational Physics*, **81**, 1-52.
8. Wang, Z.J. and Yang, H.Q. (1994). "Unsteady Flow Simulation Using a Zonal Multi-Grid Approach with Moving Boundaries." AIAA-94-0057.

# REPORT DOCUMENTATION PAGE

*Form Approved*
*OMB No. 0704-0188*



**1. AGENCY USE ONLY** (*Leave blank*)

**2. REPORT DATE**
May 1995

**3. REPORT TYPE AND DATES COVERED**
Technical Memorandum

**4. TITLE AND SUBTITLE**
A Combined Geometric Approach for Solving the Navier-Stokes Equations on Dynamic Grids

**5. FUNDING NUMBERS**
WU–505–62–52

**6. AUTHOR(S)**
John W. Slater

**7. PERFORMING ORGANIZATION NAME(S) AND ADDRESS(ES)**
National Aeronautics and Space Administration
Lewis Research Center
Cleveland, Ohio 44135–3191

**8. PERFORMING ORGANIZATION REPORT NUMBER**
E–9630

**9. SPONSORING/MONITORING AGENCY NAME(S) AND ADDRESS(ES)**
National Aeronautics and Space Administration
Washington, D.C. 20546–0001

**10. SPONSORING/MONITORING AGENCY REPORT NUMBER**
NASA TM–106919

**11. SUPPLEMENTARY NOTES**
Prepared for the Conference on Numerical Methods for Fluid Dynamics sponsored by the University of Oxford and Reading, Oxford, England, United Kingdom, April 3–6, 1995. Responsible person, John W. Slater, organization code 2610, (216) 433–8513.

**12a. DISTRIBUTION/AVAILABILITY STATEMENT**
Unclassified - Unlimited
Subject Category 02

This publication is available from the NASA Center for Aerospace Information, (301) 621–0390.

**12b. DISTRIBUTION CODE**

**13. ABSTRACT** ***(Maximum 200 words)***

A combined geometric approach for solving the Navier-Stokes equations is presented for the analysis of planar, unsteady flow about mechanisms with components in moderate relative motion. The approach emphasizes the relationships between the geometry model, grid, and flow model for the benefit of the total dynamics problem. One application is the analysis of the restart operation of a variable-geometry, high-speed inlet.

**14. SUBJECT TERMS**
Computational grids; Computational fluid dynamics; Navier-Stokes equations

**15. NUMBER OF PAGES**
9

**16. PRICE CODE**
A02

| 17. SECURITY CLASSIFICATION OF REPORT | 18. SECURITY CLASSIFICATION OF THIS PAGE | 19. SECURITY CLASSIFICATION OF ABSTRACT | 20. LIMITATION OF ABSTRACT |
|---|---|---|---|
| Unclassified | Unclassified | Unclassified | |